

Mechanical Vibration Test Equipment Design Laboratory Capacity for Automotive Industry

R. Firmansyah*, M. Sugeng

Department of Mechanical Engineering, Universitas Dian Nusantara, Jakarta, 11470, Indonesia

ARTICLE INFO

Article history:

Received date 05 September 2023

Received in revised form 17 September 2023

Accepted 24 September 2023

Keywords:

Vibration

Solidworks

Simulation

Test Equipment

Design

ABSTRACT

Vibration monitoring can also be used to find vibration levels caused by misaligned shafts and unbalanced masses, shaft misalignment of which is the root of vibration. In the UNDIRA Mechanical Engineering laboratory there is no mechanical vibration test equipment. In making the table frame and shaft, of course, it must be calculated accurately. Here the Solidworks 2017 application is used to make it easier to analyze the strength of the table frame and shaft. In simulating the strength of the Solidworks 2017 table frame and shaft, the types of materials used are Galvanized Steel and AISI 1018 and loading is carried out on the frame with a load of 7.85 N on the table frame and 2.61 N on the shaft. The simulated results obtained a stress of $7,539 \times 10^4$ (N/m²) with a displacement of 9.597 mm. The simulation results obtained safety factor values of 4.4 and 2.7. Based on Davis in the book "The Testing of Engineering Materials", the strength of the table frame of mechanical vibration test equipment is able to support the performance of the machine during use.

© 2023 JBREV. All rights reserved

INTRODUCTION

The development of technology in the fields of transportation, agriculture, communication and industry in Indonesia is growing very quickly. Almost all industrial production processes require tools to help the results of the production process. The production process will be facilitated and accelerated by the availability of these tools. However, in practice the machines related to production cannot be continuously operated. Periodic maintenance of machine performance is also required to ensure the smooth running of the production process.

Because it can slow down output, neglecting the condition of the machines will have a negative effect on this sector. The frequent occurrence of strange sounds or vibrations on the machine is one of the mistakes in using the machine that can have a negative effect. A machine that normally vibrates is different from a machine that deviates, the machine experiences wear and tear because the vibrations occur so quickly.

Although worn parts components are routinely replaced with new parts during machine overhauls

this machine wear often occurs in a short period of time.

To assess the mechanical health of machinery or equipment, vibration analysis can be applied to moving or rotating parts or machines. Vibration measurement includes the ability to take measurements without damaging or dismantling the equipment system and the ability to identify damage early, thus preventing more serious damage. Findings from vibration level measurements can be used to identify machine faults, including loose machine parts, broken gears, damaged bearings, and others.

Vibration monitoring can also be used to find vibration levels caused by misaligned shafts and unbalanced masses. Shaft misalignment, which is the root of vibration. Vibration monitoring seeks to prevent destructive and disturbing vibrations.

In the UNDIRA Mechanical Engineering laboratory there is no mechanical vibration test equipment, therefore in this study a laboratory capacity mechanical vibration test equipment was designed which can later be used as a teaching aid and the test results can be taken at any time.

According to Naibaho, W., Siahaan & Naibaho, R. (2021) motion caused by differences in

* Corresponding author.

E-mail address: rickyfirmansyah466@gmail.com

DOI: 10.59046/jbrev.v1i02.16

pressure and frequency results in vibration. Automotive engines experience a variety of vibrations, including heavy, medium, and light capacity engines [7].

According to Aritonang, Imastuti & Wulanuari (2018) the maintenance of safety and comfort is paramount in the design of four-wheeled vehicles, with the application of direct and indirect measures to ensure that the driver is not exposed to harmful interference while operating the vehicle. The suspension system is a key factor in determining driver safety and comfort. One of the main factors that can impair driver comfort and stability is vibration, which can be caused by a variety of factors including road conditions, changes in speed, and the load being carried. In cases where several factors contribute to suspension vibration, there is no damping action, resulting in severe damage to the vehicle suspension system [1].

According to Akhun (2022) a condition known as vibration comfort is one in which vibration levels do not have a negative effect on a person's health or ability to perform daily activities [6].

According to Sadiana (2016) the regular movement of objects or media in opposite directions while in a balanced state is referred to as vibration. The most common cause of vibration is when a motor is used to operate a machine or tool, this has a mechanical impact.

Newton's Law II says that the force acting on an object is equal to the product of the mass of the object by the acceleration of the object, was not originally the basis for the theoretical study of mathematical vibrations. A vibration system consists of a physical mass, a spring, a damper, and an excitation force when the workpiece vibrates [12].

According to Ikhsani (2019) The Minister of Manpower (2011) states that 0.5 meters per second squared (m/sec^2) is the threshold value (NAB) of vibration in direct or indirect contact with the entire body [16].

According to Sani & Jannah (2020) a tool that converts electrical energy into mechanical energy is a motor. In the industrial world, electric motors are usually used in various household appliances and machine tools. The majority of industrial machinery and household appliances that we encounter usually use AC (alternating current) electric motors [13].

According to Purwanto, Faizin & Mashudi (2016) a rotating engine shaft is a component that transfers power from one engine to another [10].

According to Raharjo in Lubis *et al.*, (2021) glide bearings/journal bearings are a type of alternative bearing for rolling bearings, and are usually used in machines with rotating shafts. The bearing itself consists of a bushing or slide, which is held in place by the bearing housing and rotates in the bushing hole along with the shaft or journal it

supports [3].

According to Rizal & Suhadi (2010), the gliding bearing will last a long time and have a good wear resistance. This method is employed not just to produce pores but also because it is capable of producing intricately shaped components with excellent precision, little energy usage, and economical raw material usage. Minimal energy use and effective raw material use [2].

According to Shita (2021), a coupling can be described as a component used to connect two shafts at their ends to provide continuous power and rotation. From the prime mover (electric motor, combustion motor, or turbine), power and rotation are transmitted [15].

Nasution & Hidayat (2018) state that bolts and nuts are important fasteners in machinery. Because nuts and bolts are used to connect or tighten parts to each other, especially in machines and also nuts and bolts serve to secure the electric motor to the machine frame, preventing accidents or damage to the machine [8].

On the other side, Basori, Marsudi & Saputra (2018) state that on machines, nuts and bolts play an important role as fasteners. To hold two pieces of metal or plate together, nuts and bolts are used [14].

According to Mayasari & Basuki (2021), hollow iron is a type of iron in the form of a square pipe. This material is considered high quality and is ideal for use in the construction of ceiling iron frames and partition walls of houses and buildings [5].

According to Wijaya and Kusumarini (2015), strong materials like hollow iron are perfect for table legs. The hollow iron that is utilized is 4 cm by 4 cm in dimension [4].

According to Deti and Mulyono (2017), Plywood is a processed wood product made from solid wood, often known as multiplex or triplex. This product is constructed with veneers, which are thin sheets of wood. After positioning each veneer such that the fibers overlap in the direction that they cross, it is bonded together with intense pressure. Additionally, plywood comes in thicknesses ranging from 0.8 mm to 25 mm [9].

Romiyadi & Irwan (2020) state that a device called a vibration meter is used to detect vibrations on various items, such as motors, pumps, and other vibrating objects, especially in the industrial field. The vibration sensor or magnetic base of the vibration meter is attached to the machine or item being monitored, and the magnetic base then transmits data via cable to the reader unit. As a result, the vibration meter displays the vibration amplitude value for the monitored machine or object [11].

A popular design application for working on machine design, building design, product design, and other technical tasks are Solidworks 2017. The capabilities in Solidworks software are used to

compute and evaluate design outcomes, including impacts of temperature, strain, and stress, among other things. Since Solidworks is a parametric feature-based modeling program, the design process of a product or design can be greatly facilitated by the ability to modify all objects and relationships between geometrics even after the geometry has been completed, eliminating the need to start from scratch [17].

METHODOLOGY

The design method is carried out by several methods, namely literature study and observation, the tools used in the design include hardware and software, material selection, design calculations using solidworks software, making machine component designs and table frames, making vibration test equipment based on design, simulation testing.

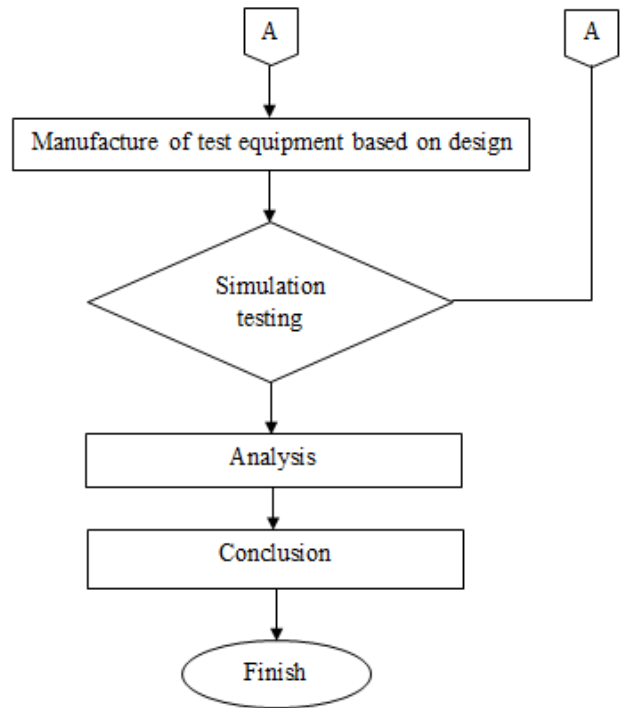
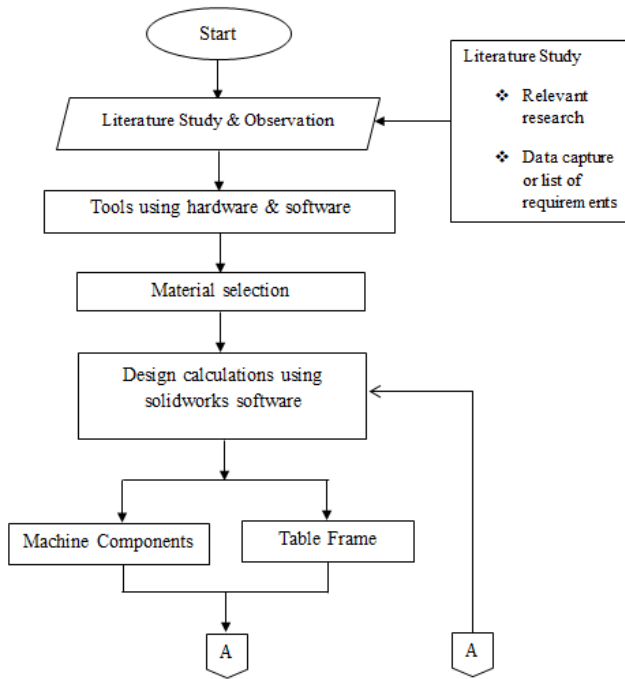


Fig. 1. Flowchart of design method.

RESULTS AND DISCUSSION

Table Frame Static Simulation Results

Stress simulation results on the table frame with a load of 7.85 N (0.8 kg) can be seen from the results of Fig. 2 below.

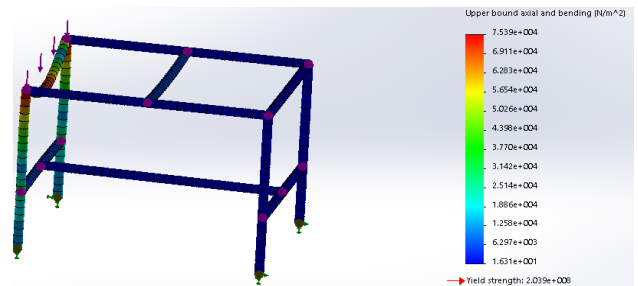


Fig. 2. Stress simulation.

- In blue the shape of the table leg at 1.631 is where the voltage starts to react and things still look normal.
- In green the shape of the table leg at 3.770 is where the voltage has reacted and changed.
- In the red color the shape of the table leg at 7.539 is where the total stress forms so that the stress is very hard.

Displacement simulation results on the table frame with a load of 7.85 N (0.8 kg) can be seen from the results of Fig. 3 below.

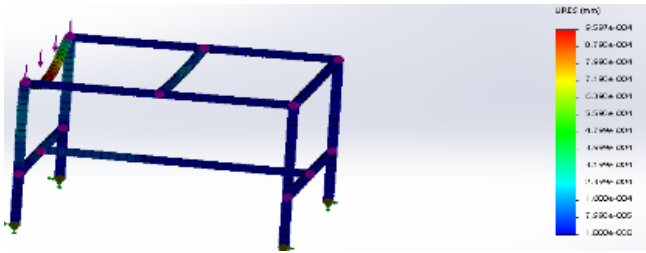


Fig. 3. Displacement simulation.

- In blue, the shape of the table leg at 1,000 is where the deformation starts to react and things still look normal.
- In the green color the shape of the table leg at 5,598 is where the shape change begins to react and change.
- In red the shape of the table leg at 9,597 is where the total shape change so that the shape is increasingly curved.

The factor of safety simulation results on the table frame with a load of 7.85 N (0.8 kg) can be seen from the results of Fig. 4 below.

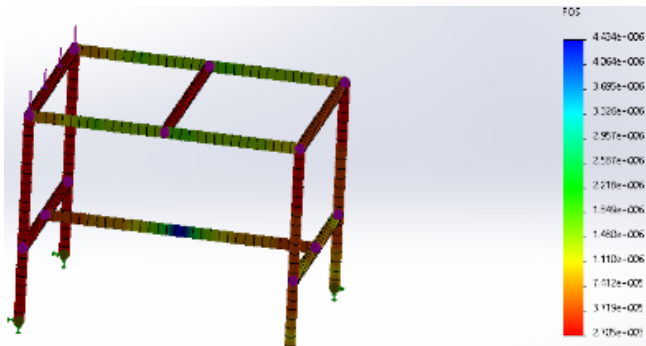


Fig. 4. Factor of safety simulation.

- In red, the shape of the table leg at 2.7 is where the safety factor starts to react and things still look normal.
- In green the shape of the table leg at 2.9 is where the safety factor changes begin to react and increase.
- In the blue color the shape of the table leg at 4.4 is where the safety factor changes in total form so that the safety factor level increases.

Shear force simulation results on the table frame with a load of 7.85 N (0.8 kg) can be seen from the results of Fig. 5 below.

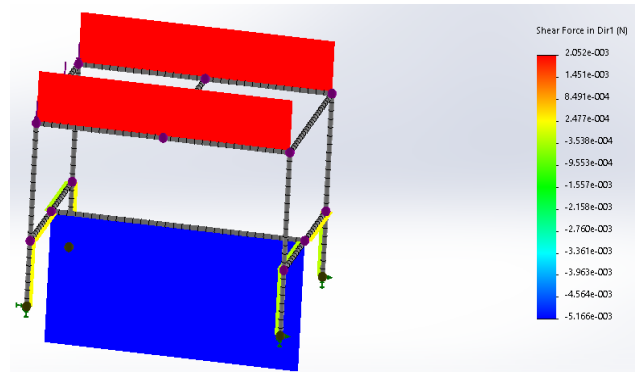


Fig. 5. Shear force simulation.

- In red, the shape of the table leg at 2.052 is where the shear stress starts to react and things still look normal.
- In green the shape of the table leg at 3.538 is where the shear stress changes have reacted and increased towards the left.
- In the blue color the shape of the table leg at 5.166 is where the total shear stress changes so that the shear stress level increases towards the right.

Static Simulation Result of 12 mm Shaft

The results of the factor of safety 01 simulation on the shaft with a load of 2.61 N (0.266 kg) can be seen from the results of Fig. 6 below.

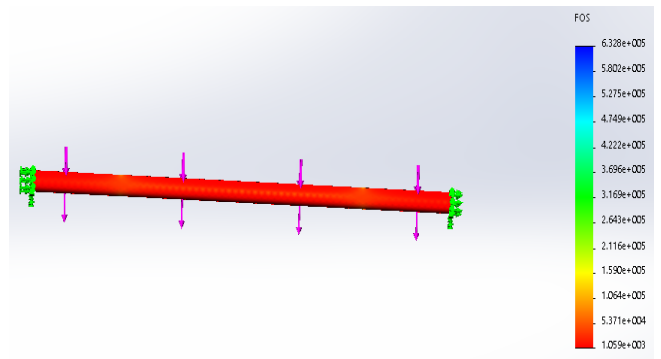


Fig. 6. Factor of safety 01 simulation.

- In red the factor of safety value of the shaft shape at 1.1 is where the change in the Factor Of Safety value of the shaft reaches the minimum point.
- In green the factor of safety value of the shaft at 3.7 is where the change in the factor of safety value of the shaft starts to increase.
- In blue the factor of safety value of the shaft at 6.3 is where the change in the factor of safety value of the shaft reaches its maximum point.

The simulation results of factor of safety 02 on the shaft with a load of 2.61 N (0.266 kg) can be seen from the results of Fig. 7 below.

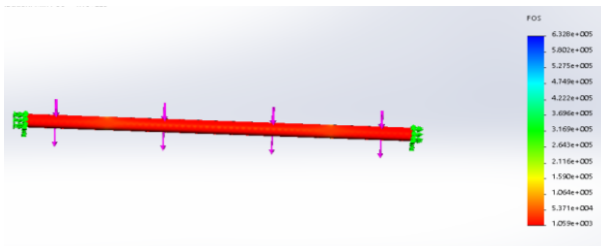


Fig. 7. Factor of safety 02 simulation.

- In red the factor of safety value of the shaft shape at 1.1 is where the change in the factor of safety value of the shaft reaches the minimum point.
- In green the factor of safety value of the shaft at 3.7 is where the change in the factor of safety value of the shaft starts to increase.
- In blue the factor of safety value of the shaft at 6.3 is where the change in the factor of safety value of the shaft reaches its maximum point.

Linear Dynamic Simulation Results of 12 mm Shaft

Stress simulation results on the shaft with a load of 2.61 N (0.266 kg) can be seen from the results of Fig. 8 below.

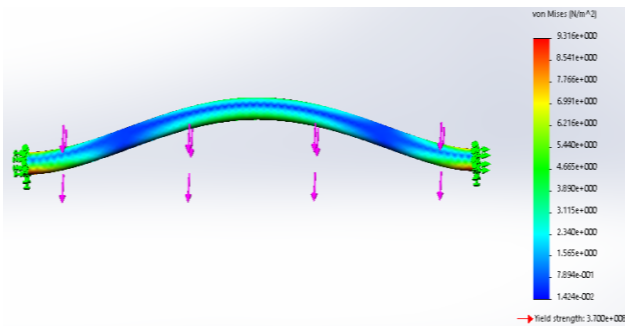


Fig. 8. Stress simulation.

- In blue the shape of the shaft at 1.424 is where the stress starts to react and things still look normal.
- In green the shape of the shaft at 5.442 is where the stress has reacted and changed.
- In red the shape of the shaft at 9.316 is where the total stress forms so that the stress is very hard.

Displacement simulation results on the shaft with a load of 2.61 N (0.266 kg) can be seen from the results of Fig. 9 below.

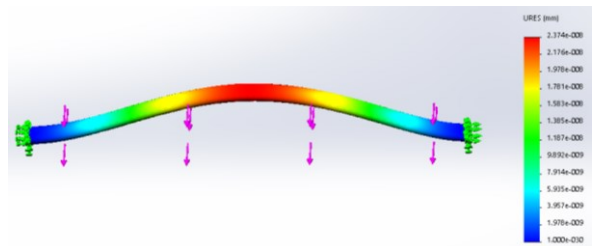


Fig. 9. Displacement Simulation.

- In blue the shape of the shaft at 1,000 is where the shaft shape changes begin to react and things still look normal.
- In green the shape of the shaft at 1,187 is where the change in the shape of the shaft has begun to react and change.
- In red the shape of the shaft at 2,374 is where the shaft shape changes completely so that the shaft shape is increasingly curved.

Strain simulation results on the shaft with a load of 2.61 N (0.266 kg) can be seen from the results of Fig. 10 below.

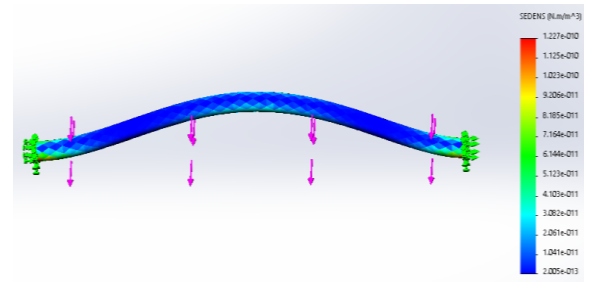


Fig. 10. Strain simulation.

- In red the shape of the shaft at 1.227 is where the change in the shape of the shaft begins to react and things still look normal.
- In green the shape of the shaft at 6.144 is where the change in the shape of the shaft has begun to react and experience changes in length.
- In blue the shape of the shaft at 2.005 is where the change in the length of the total shaft shape so that the shaft shape is getting longer.

Velocity simulation results on the shaft with a load of 2.61 N (0.266 kg) can be seen from the results of Fig. 11 below.

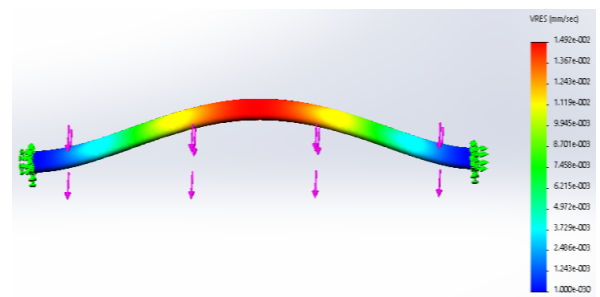


Fig. 11. Velocity simulation.

- In blue the velocity value of the shaft shape at 1,000 is where the change in the velocity value of the shaft reaches the minimum point.
- In orange the shaft velocity value at 1,119 is where the change in shaft velocity value begins to increase.
- In red the shaft velocity value at 1.492 is where the change in shaft velocity value reaches the maximum point.

Acceleration simulation results on the shaft with a load of 2.61 N (0.266 kg) can be seen from the results of **Fig. 12** below.

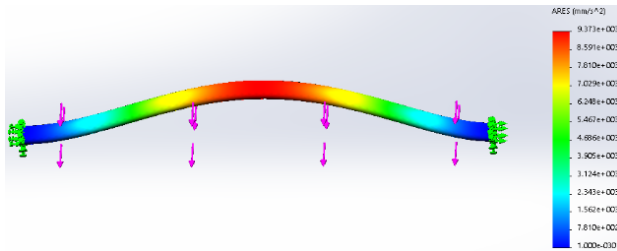


Fig. 12. Acceleration simulation.

- In blue the acceleration value of the shaft shape at 1.000 is where the change in the acceleration value of the shaft reaches its minimum point.
- In green the acceleration value of the shaft at 4.686 is where the change in the acceleration value of the shaft starts to increase.
- In red the acceleration shaft value at 9.373 is where the change in the acceleration shaft value reaches its maximum point.

Solidworks Motion Velocity Simulation Results

The results of the solidworks motion velocity simulation on the shaft with a load of 2.61 N (0.266 kg) and 2600 rpm obtained an increase in value of 0.015 mm/sec and a decrease of -0.012 mm/sec with a time of 18 seconds, can be seen from the results of **Fig. 13** below.

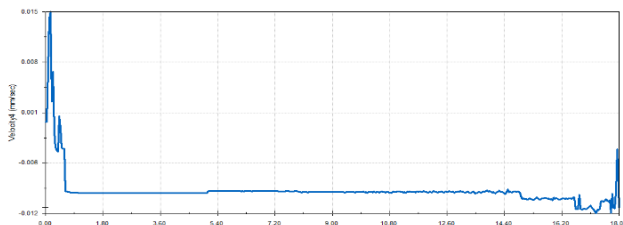


Fig. 13. Velocity result 2600 rpm.

Solidworks motion velocity simulation results on the shaft with a load of 2.61 N (0.266 kg) and 2850 rpm obtained an increase in value of 0.063 mm/sec and a decrease of -0.012 mm/sec with a time of 18 seconds, can be seen from the results of **Fig. 14** below.

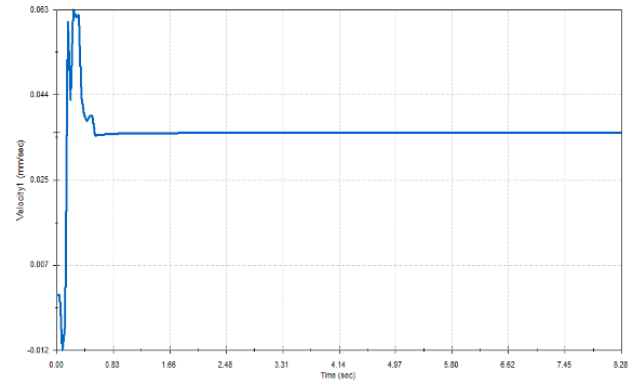


Fig. 14. Velocity result 2850 rpm.

The results of the solidworks motion velocity simulation on the shaft with a load of 2.61 N (0.266 kg) and 2,900 rpm obtained an increase in value of 40.427 mm/sec and a decrease of -51.268 mm/sec with a time of 18 seconds, can be seen from the results of **Fig. 15** below.

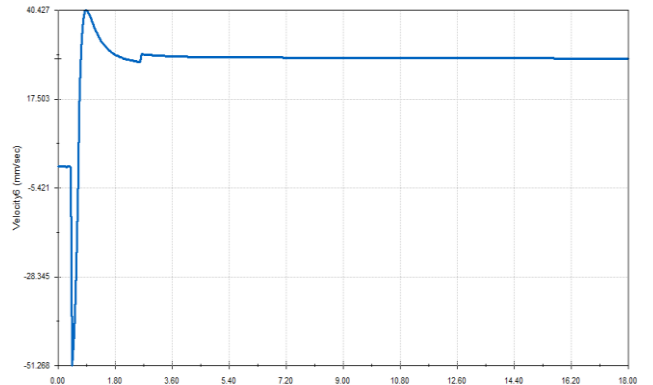


Fig. 15. Velocity result 2900 rpm.

Solidworks Motion Linear Acceleration Simulation Results

The results of the solidworks motion linear acceleration simulation on the shaft with a load of 2.61 N (0.266 kg) and 2,600 rpm obtained an increase in value of 225 mm/sec² and a decrease of -15 mm/sec² with a time of 18 seconds, can be seen from the results of **Fig. 16** below.

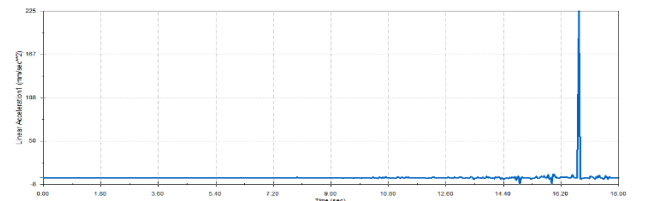


Fig. 16. Linear acceleration result 2600 rpm.

The results of the solidworks motion linear acceleration simulation on the shaft with a load of 2.61 N (0.266 kg) and 2850 rpm obtained an increase in value of 42 mm/sec² and a decrease of -14 mm/sec² with a time of 18 seconds, can be seen from the results of **Fig. 17** below.

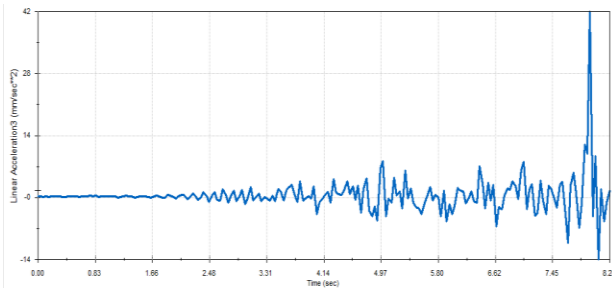


Fig. 17. Linear acceleration result 2850 rpm.

The results of the solidworks motion linear acceleration simulation on the shaft with a load of 2.61 N (0.266 kg) and 2,900 rpm obtained an increase in value of 14,536.427 mm/sec² and a decrease of -13,106 mm/sec² with a time of 18 seconds, can be seen from the results of Fig. 18 below.

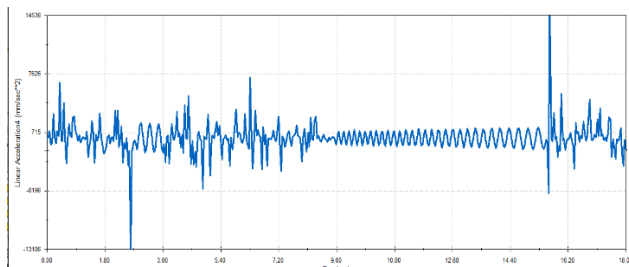


Fig. 18. Linear acceleration result 2900 rpm.

CONCLUSION

From the research that has been done and analyzing the data obtained, the following conclusions can be drawn:

1. The table frame design using galvanized steel material that has been made is safe to withstand loads up to 0.8 kg, this is because the safety factor value is 2.7 - 4.4.
2. The shaft design using ST 41/AISI 1018 material that has been made is safe to withstand loads up to 0.266 kg, this is because the safety factor value is 1.1 - 6.3.
3. In solidworks simulation, especially in dynamic simulation with the same material and load used as in static simulation, the minimum velocity value of 1,000 (mm/sec) and a maximum of $1,492 \times 10^2$ (mm/sec) are obtained, for a minimum acceleration value of $1,000 \times 10^1$ (mm/s²) and a maximum of $9,373 \times 10^3$ (mm/s²) so that it is safe when used.
4. In solidworks motion, the highest value is obtained from the three rpm and the highest value is in velocity with 2900 rpm of 40.427 mm/sec and a decrease of 51.268 mm/sec while in linear acceleration the highest value at 2900 rpm is 14,536.427 mm/sec² and a decrease of -13,106 mm/sec² so it is safe to use.

ACKNOWLEDGEMENT

This work is supported by Universitas Dian Nusantara in fiscal year 2023.

AUTHOR CONTRIBUTION

R. Firmansyah and M. Sugeng contributed equally as the main contributors of this paper. All authors read and approved the final version of the paper.

REFERENCES

- [1] Aritonang, S., Imastuti, I., & Wuluanuari, P. H. (2018). Analisis Kerusakan Yang Disebabkan Oleh Vibrasi Pada Sistem Suspensi Kendaraan Roda Empat. *Jurnal Teknologi Daya Gerak*, 1(1).
- [2] Rizal, S., & Suhadi, A. (2010). Identifikasi karakteristik mekanis bantalan luncur motor starter dari serbuk tembaga alumunium. *Jurnal Sains dan Teknologi Indonesia*, 12(3), 174-179.
- [3] Lubis, F., Pane, R., Lubis, S., Siregar, M. A., & Kusuma, B. S. (2021). Analisa Kekuatan Bearing Pada Prototype Belt Conveyor. *Jurnal MESIL (Mesin Elektro Sipil)/Journal MESIL (Machine Electro Civil)*, 2(2), 51-57.
- [4] Wijaya, C., & Kusumarini, Y. (2015). Portable Folding Furniture untuk Interior Apartemen Tipe Studio. *Intra*, 3(2), 9-17. Yogyakarta.
- [5] Mayasari, A., & Basuki, B. (2021). Analisa Daerah Haz Besi Hollow Terhadap Variasi Elektroda. *Matrik: Jurnal Manajemen dan Teknik Industri Produksi*, 22(1), 45-54.
- [6] Nafan Akhun. (2022). *Buku Pintar Standar Akreditasi RS: Standar Akreditasi Rumah Sakit Dasar*. Khulyan Publisher : Jakarta.
- [7] Naibaho, W., Siahaan, S., & Naibaho, R. (2021). Analisa Perbandingan Condition Pada Mobil Daihatsu Taruna Terhadap Karakteristik Getaran Berdasarkan Time Domain. *Jurnal MESIL (Mesin Elektro Sipil)/Journal MESIL (Machine Electro Civil)*, 2(1), 25-35. Putaran Mesin Untuk Kompresor Air
- [8] Nasution, A. Y., & Hidayat, G. (2018). Rancang bangun alat pengaduk adonan bubur organik kapasitas 7 liter untuk industri umkm. *SINTEK JURNAL: Jurnal Ilmiah Teknik Mesin*, 12(2), 113-124.
- [9] Deti, L. K., & Mulyono, H. (2017). Analisis Dan Perancangan Sistem Informasi Penjualan Dan Pemesanan Plywood Berbasis Web Pada PT. Kumpeh Karya Lestari Jambi. *Jurnal Manajemen Sistem Informasi*, 2(1), 303-317.
- [10] R. Edy Purwanto., Akhmad Faizin, Imam Mashudi. 2016. *Elemen Mesin 1*. Polinema Press: Malang.

- [11] Romiyadi, R., & Irwan, P. (2020). The Effect of Misalignment to Vibration, Electric Current and Shaft Rotation Speed on The Coupling Transmision. *Jurnal Teknik Mesin*, 10(2), 73-78.
- [12] Sadiana, R. (2016). Analisis Respon Sistem Getaran Pada Mesin Torak. *Jurnal Ilmiah Teknik Mesin*, 4(2), 41-46.
- [13] Sani, A., & Jannah, E. E. N. (2020). Purwarupa pengendali kecepatan motor induksi 1 fasa via android. *Jurnal Integrasi*, 12(2), 88-91.
- [14] Saputra, B. R. (2018). Perancangan Mesin Perontok Jagung Dengan Kapasitas Produksi 300 Kg/Jam. *Jurnal Konversi Energi dan Manufaktur*, 5(1), 7-14.
- [15] Shita, U. (2021). Studi Eksperimental Distribusi Tegangan Baut Pada Kopling Tetap Jenis Flens. *Almikanika*, 2(4), 154-161.
- [16] Ikhssani, A. (2019). Physical Potential Hazards On The Palm Oil Processing Of PT. Perkebunan Nusantara VII 2019. *Preventif: Jurnal Kesehatan Masyarakat*, 10(2), 95-103.
- [17] Adi, I. N. A., Dantes, K. R., & Nugraha, I. N. P. (2018). Analisis Tegangan Statik pada Rancangan Frame Mobil Listrik Ganesha Sakti (GASKI) Menggunakan Software SolidWorks 2014. *Jurnal Pendidikan Teknik Mesin Undiksha*, 6(2), 113-12